Journal of Experimental and Theoretical Physics, Vol. 97, No. 5, 2003, pp. 989–995.
Translated from Zhurnal Éksperimental'noĭ i Teoreticheskoĭ Fiziki, Vol. 124, No. 5, 2003, pp. 1103–1111.

SOLIDS
Structure

Magnetic and Electrical Properties of $Fe_{1.91}V_{0.09}BO_4$ Warwickite

A. D. Balaev[a], O. A. Bayukov[a], A. D. Vasil'ev[a], D. A. Velikanov[a], N. B. Ivanova[b], N. V. Kazak[a,*], S. G. Ovchinnikov[a], M. Abd-Elmeguid[c], and V. V. Rudenko[a]

[a]*Kirensky Institute of Physics, Siberian Division, Russian Academy of Sciences, Krasnoyarsk, 660036 Russia*
[b]*Krasnoyarsk State Technical University, Krasnoyarsk, 660074 Russia*
[c]*Physikalisches Institut II, Universität zu Köln, 50937 Köln, Germany*
**e-mail: nat@iph.krasn.ru; sgo@iph.krasn.ru*
Received April 16, 2003

Abstract—We have performed a complex investigation of the structure and the magnetic and electrical properties of a warwickite single crystal with the composition $Fe_{1.91}V_{0.09}BO_4$. The results of Mössbauer measurements at $T = 300$ K indicate that there exist "localized" (Fe^{2+}, Fe^{3+}) and "delocalized" ($Fe^{2.5+}$) states distributed over two crystallographically nonequivalent positions. The results of magnetic measurements show that warwickite is a *P*-type ferrimagnet below $T = 130$ K. The material exhibits hopping conductivity involving strongly interacting electrons. The experimental data are analyzed in comparison to the properties of the initial (unsubstituted) Fe_2BO_4 warwickite. The entire body of data on the electric conductivity and magnetization are interpreted on a qualitative basis. © *2003 MAIK "Nauka/Interperiodica".*

1. INTRODUCTION

Most transition metal oxyborates with the general chemical formula $M^{2+}M^{3+}BO_4$ crystallize in an orthorhombic structure of warwickite ($Mg_{1.5}Ti_{0.5}BO_4$) representing a system of linear, weakly interacting ribbons comprising two internal and one external chains in which octahedrally coordinated divalent and trivalent transition metal atoms are randomly distributed over nonequivalent crystallographic positions of two types. In recent years, these compounds have drawn the attention of researchers due to an unusual combination of properties inherent in significantly disordered, strongly correlated electron systems [1–6].

From the theoretical standpoint, by studying the Heisenberg one-dimensional chains with integer or half-integer spins, it is possible to assess the influence of disorder on the spectrum of excitations, calculate the thermodynamic parameters, and describe the properties of the ground state. Experimentally, it is possible to observe a number of interesting phenomena such as temperature-induced magnetic transitions, unusual magnetization and heat capacitance curves, and the Mott transition from the delocalized to localized state in the conductivity. In addition, the possibility of synthesizing warwickites with most transition elements opens wide possibilities for a systematic investigation into their physical properties.

To the present, some monometallic (Fe_2BO_4 [4], Mn_2BO_4) [6]) and a series of bimetallic oxoborates of the $(M,M')BO_4$ type have been synthesized, where either both M and M' are transition elements ($FeCoBO_4$ [7], $FeMnBO_4$ [8], $ScMnBO_4$ [2]) or M can be a nonmagnetic alkali earth metal such as Mg or Ca [1].

From the standpoint of magnetic order, bimetallic oxoborates with a nonmagnetic metal M represent Heisenberg one-dimensional antiferromagnetic chains with integer or half-integer spins. These compounds have been theoretically and experimentally studied to a certain extent by Continentino *et al.* [9–11]. Systems with half-integer spin were represented by $MgTiBO_4$, and those with integer spins, by $MgVBO_4$. The choice of vanadium as a transition metal is related to large dimensions of its 3*d* orbitals, which accounts for the Heisenberg nature of exchange interactions. The results of investigations showed that behavior of the magnetic susceptibility in a broad temperature interval and the magnetization curves of these systems obey a power law characteristic of strongly disordered spin chains, both with $S = 1/2$ and with $S = 1$. It was demonstrated that $MgVBO_4$ exhibits a phase transition to the spin glass state at $T = 6$ K.

In this paper, we present $Fe_{1.91}V_{0.09}BO_4$ warwickite, a new compound with two magnetic 3*d* metal ions. The magnetic and electrical properties of this compound will be described in comparison to a rather thoroughly studied Fe_2BO_4 warwickite (see, e.g., [4, 12–14]). The most interesting features of this initial (unsubstituted) compound are the phase transitions of three types: a structural transition from monoclinic to orthorhombic structure at $T = 317$ K is accompanied by an electron transition from the semiconductor–semiconductor state (related to delocalization of the charge carriers) and is

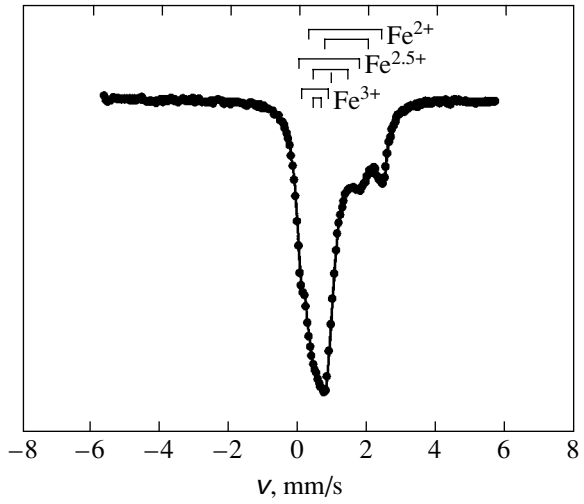

Fig. 1. The room-temperature Mössbauer spectrum of $Fe_{1.91}V_{0.09}BO_4$ warwickite.

followed by the magnetic phase transition from the paramagnetic to *P*-type ferrimagnetic state at $T = 155$ K.

2. SAMPLE PREPARATION AND EXPERIMENTAL METHODS

$FeVBO_4$ single crystals were grown using a solution melt technology in the Fe_2O_3–V_2O_3–B_2O_3–(70PbO + 30PbF_2, wt %) system with intermediate cooling of the solution-melt from 900 to 780°C. Attfield *et al.* [4] met serious difficulties in their attempts to grow Fe_2BO_4 single crystals from a solution-melt, for which reason they used solid-phase synthesis and obtained only polycrystalline samples incorporating some other phases (removed by magnetic methods). We have succeeded in obtaining $FeVBO_4$ crystals possessing a regular shape and smooth surface. The samples had the form of needles (whiskers) with a length of up to 1 cm and a thickness of 0.10–0.15 mm.

Elemental composition of the grown samples was determined by energy-dispersive X-ray spectroscopy (EDAX ZAF quantification procedure), which showed that the relative content of iron and vanadium is 95.42 and 4.58 at. %, so that a formula unit of the substituted warwickite is $Fe_{1.91}V_{0.09}BO_4$.

X-ray diffraction was studied on a setup of the D8 ADVANCE type using CuK_α radiation (λ = 1.5406 Å). Room-temperature scans over $2\theta = 13.4°$–89.7° showed evidence for an orthorhombic structure (*Pnam*). The lattice parameters of our samples are presented in Table 1 in comparison to the data for Fe_2BO_4 reported in [15]. The unit cell volume of $Fe_{1.91}V_{0.09}BO_4$ is 274.82 Å^3, which virtually coincides with the value for Fe_2BO_4 (275.02 Å^3). However, in contrast to the room-temperature orthorhombic structure of $Fe_{1.91}V_{0.09}BO_4$, Fe_2BO_4 exhibits pronounced monoclinic distortions.

Table 1. Crystal lattice parameters of substituted and unsubstituted warwickites

	a, Å	*b*, Å	*c*, Å	β	*V*, Å^3
$Fe_{1.91}V_{0.09}BO_4$	3.1727	9.3831	9.2317	89.993	274.84
Fe_2BO_4	3.1688	9.3835	9.2503	90.22	275.02

The temperature and field dependences of magnetization were measured on a vibrating-sample magnetometer with a superconducting coil. The zero-field magnetization measurements were performed using a SQUID magnetometer.

The Mössbauer spectra were obtained using a ^{57}Co(Cr) source. The measurements were performed on single crystal powders of $Fe_{1.91}V_{0.09}BO_4$ with a linear density of 5–10 mg/cm and a natural room-temperature iron content.

The dc resistivity measurements in a range of temperatures $T = 90$–430 K were performed in a two-contact scheme. High resistances were measured using a teraohmmeter E6-13A capable of measuring resistances up to 10^{13} Ohm. The contacts were made of an indium-based paste and their ohmic behavior was checked by measuring current–voltage characteristics. The temperature was measured by a copper–constantan thermocouple placed immediately at a sample. The samples were heated and cooled at a rate of 1 K/min, so as to avoid parasitic temperature gradients.

3. MÖSSBAUER MEASUREMENTS

The room-temperature Mössbauer spectrum of a $Fe_{1.91}V_{0.09}BO_4$ single crystal (Fig. 1) represents a superposition of several quadrupole doublets. The resolution of spectral lines is lower than that in the spectrum of unsubstituted warwickite [4, 14], which can be related both to a decrease in the electron delocalization temperature for Fe^{2+}–Fe^{3+} and to the vanadium additive.

Figure 2 shows the probability distribution functions of the quadrupole splitting, $P(E_Q)$, for three valence states of iron (Fe^{3+}, $Fe^{2.5+}$, Fe^{2+}) in the spectrum of substituted warwickite. These functions possess a qualitative character, since the fitting parameters (isomer shifts) were the same for all distributions. As can be seen, Fe^{3+} and Fe^{2+} cations occupy nonequivalent (with respect to local environment) crystallographic positions I and II, respectively, while $Fe^{2.5+}$ cations possess local environments of three types differing by the values of quadrupole splitting. Thus, the observed spectrum of $Fe_{1.91}V_{0.09}BO_4$ should be approximated by seven quadrupole doublets. An analogous model was used [14] for interpreting the spectrum of unsubstituted Fe_2BO_4 warwickite.

The hyperfine structure parameters determined upon fitting a model curve to the experimental spec-

trum by the least square technique assuming the Lorentzian line shape are presented in Table 2. The isomer shifts of Fe^{2+}(I, II) and Fe^{3+}(I, II) are typical of the localized states of these cations occurring in a high-spin state with octahedral oxygen coordination. The isomer shifts of $Fe^{2.5+}$(I, IIa, IIb) are characteristic of a mixed valence of Fe^{2+} and Fe^{3+} cations, which appears as a result of the fast electron exchange between these ions. The ratio of the isomer shifts indicates that the electron density on an iron nucleus is higher in position II than in position I. At the same time, the values of quadrupole splitting show that the coordination octahedron in position II is more distorted than that in position I. A relatively high symmetry in position I allows us to assign the $Fe^{2.5+}$(I) singlet to this position, and the $Fe^{2.5+}$(IIa) and $Fe^{2.5+}$(IIb) doublets, to nonequivalent states in position II.

The distribution of Fe^{2+}, $Fe^{2.5+}$, and Fe^{3+} ions over crystallographic positions I and II, as determined from the Mössbauer measurements, allows us to write the formula of vanadium-substituted warwickite as follows:

$$(Fe^{3+}_{0.383}Fe^{2+}_{0.313}Fe^{2.5+}_{0.299})_I(Fe^{3+}_{0.278}Fe^{2+}_{0.279}Fe^{2.5+}_{0.359}V^{2+}_{0.09})_{II}BO_4.$$

The deficit of cations in position I (~0.005) according to this formula is small compared to the content of vanadium in the crystal and may be related to experimental uncertainty. Thus, the experimental data show that vanadium occupies only positions II in the given warwickite structure. Taking into account the condition of electroneutrality, the formal valence of vanadium in this compound is 2+.

A comparison of the cation distribution established in the crystal studied to that in the unsubstituted warwickite [13, 14],

$$(Fe^{3+}_{0.36}Fe^{2+}_{0.38}Fe^{2.5+}_{0.26})_I(Fe^{3+}_{0.36}Fe^{2+}_{0.38}Fe^{2.5+}_{0.26})_{II}BO_4,$$

suggests that vanadium replaces Fe^{2+} ions in positions II, after which the total amount of iron ions subjected to fast electron exchange in the crystal increases from 0.52 (in Fe_2BO_4) to 0.66 (in $Fe_{1.91}V_{0.09}BO_4$) per formula unit. Therefore, the introduction of vanadium into the warwickite crystal changes the ratio of delocalized atoms in positions I and II. In particular, the presence of vanadium in sublattice II increases the number of delocalized atoms in this sublattice from 0.26 (in Fe_2BO_4) to 0.359 (in $Fe_{1.91}V_{0.09}BO_4$) per formula unit. This increase is significantly greater than that in sublattice I (from 0.26 to 0.299 per formula unit).

Apparently, vanadium entering into a sublattice may induce some ordering of the cations with different valences in this sublattice (similar to the ordering effect observed in manganese-containing warwickite [6]), for example, of the type $V–Fe^{2+}–Fe^{3+}–V–Fe^{2+}–Fe^{3+}$. Probably, the two nonequivalent states, $Fe^{2.5+}$(IIa) and $Fe^{2.5+}$(IIb), appear as a result of this process.

4. MAGNETIZATION MEASUREMENTS

Figure 3 shows the temperature dependence of magnetization, $M(T)$, in $Fe_{1.91}V_{0.09}BO_4$ warwickite measured with a SQUID magnetometer in zero magnetic field. Figure 4 presents an $M(T)$ curve measured with a vibrating-sample magnetometer for an external magnetic field of H = 1 kOe applied parallel to the a axis of a needle crystal. A broad maximum observed in the region of T = 60 K is characteristic of a P-type ferrimagnetic order, while a transition to the paramagnetic state takes place at T = 130 K. The $M(T)$ curve in Fig. 3 displays a feature (step) at T = 120 K, which was previously reported [12–14] for Fe_2BO_4. Continentino *et al.* [12] assigned this feature to the Verwey transition in an impurity phase of magnetite (Fe_3O_4), while Douvalis *et al.* [13, 14] pointed to the existence of a series of transitions in the 45–130 K range and attributed these features to different temperature dependences of mag-

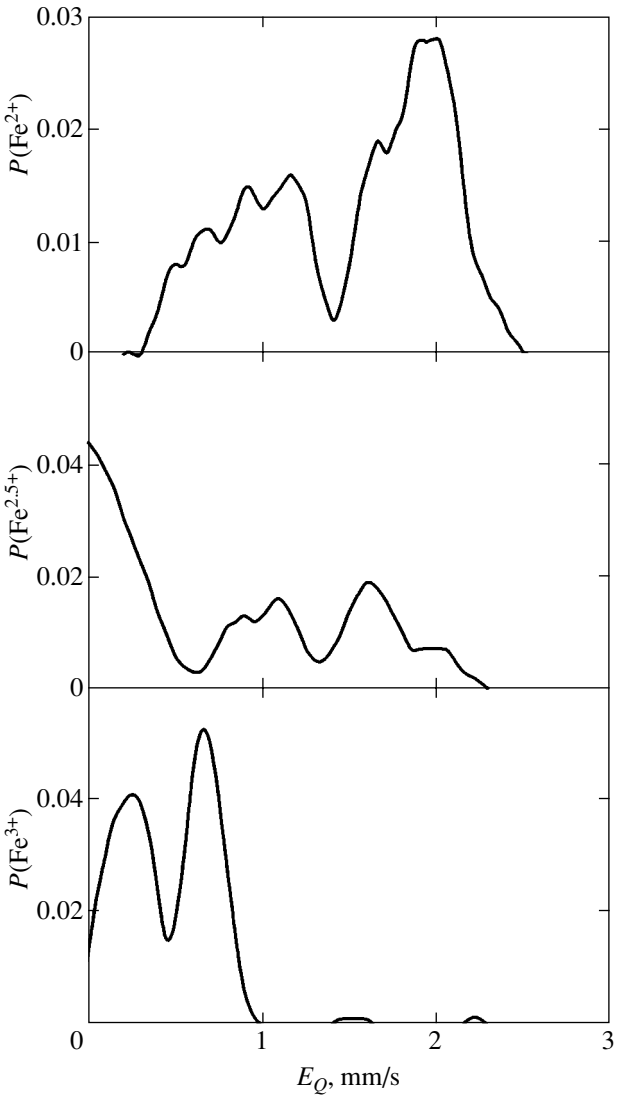

Fig. 2. The probability distribution functions of quadrupole splitting in $Fe_{1.91}V_{0.09}BO_4$ warwickite.

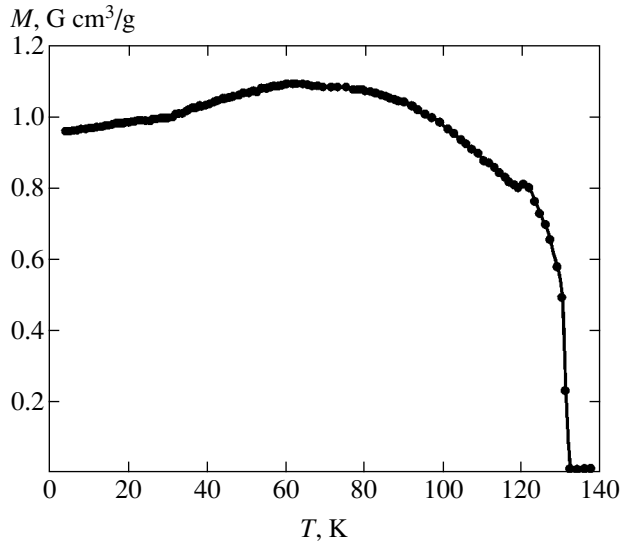

Fig. 3. The temperature dependence of magnetization for $Fe_{1.91}V_{0.09}BO_4$ in a zero field.

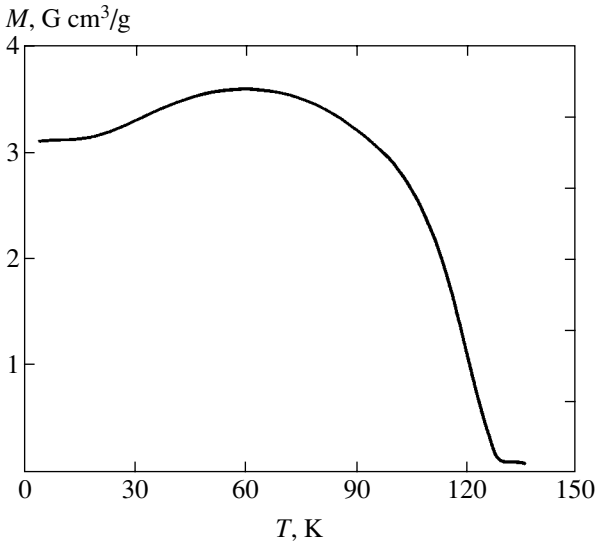

Fig. 4. The temperature dependence of magnetization for $Fe_{1.91}V_{0.09}BO_4$ in a field of $H = 1$ kOe.

netization for the two sublattices in unsubstituted Fe_2BO_4. In our experiments, neither magnetic measurements nor X-ray diffraction on high-quality single crystals showed evidence of the presence of magnetite impurity. Apparently, the feature at $T = 120$ K is inherent in $Fe_{1.91}V_{0.09}BO_4$ warwickite and probably in Fe_2BO_4 as well.

The $M(T)$ curve in Fig. 4 exhibits, generally, the same character as that reported fir Fe_2BO_4 [12]. However, the presence of vanadium ions in the structure even in small amounts decreases the magnetic transition temperature. A long-range magnetic order in $Fe_{1.91}V_{0.09}BO_4$ is established at $T = 130$ K, whereas the same transition in Fe_2BO_4 takes place at 155 K. The same trend was observed previously in a series of solid solutions of the $Fe_{1-x}V_xBO_3$ system [16].

Figure 5 presents the magnetization curves of a $Fe_{1.91}V_{0.09}BO_4$ single crystal at 4.2 and 100 K, showing the presence of an uncompensated magnetic moment of 0.1 μ_B per formula unit. This value is greater than that reported for Fe_2BO_4 (0.06 μ_B) [4]. At $H > 1$ T, the $M(H)$ plots represent linear dependences without any features, which corresponds to rotation of the magnetization vectors of sublattices toward the external magnetic field direction. As can be seen from Fig. 5, there is a nonzero magnetization in the region of small fields, which is probably related to the presence of a magnetic crystallographic anisotropy.

Table 2. Hyperfine structure parameters determined from the Mössbauer spectrum of $Fe_{1.91}V_{0.09}BO_4$ warwickite

	$\delta(\alpha_{Fe})$, mm/s	ΔE_Q, mm/s	Γ, mm/s	A, %
Fe^{3+}(I)	0.378	0.192	0.350	20
Fe^{3+}(II)	0.287	0.743	0.286	14.5
Fe^{2+}(I)	1.196	1.236	0.576	16.4
Fe^{2+}(II)	1.192	2.147	0.344	14.6
$Fe^{2.5+}$(I)	0.76	–	0.504	15.6
$Fe^{2.5+}$(IIa)	0.75	1.006	0.583	13.3
$Fe^{2.5+}$(IIb)	0.702	1.736	0.304	5.5

5. ELECTRIC RESISTANCE

On the whole, the temperature dependence of the electric resistance observed for $Fe_{1.91}V_{0.09}BO_4$ single crystals (Fig. 6) is typical of 3*d* metal borates such as Fe_2BO_4, VBO_3, and $Fe_{1-x}V_xBO_3$ [16], exhibiting a sharp increase in the resistivity and "dielectrization" of the sample at low temperatures. Features of the electron systems behavior in these materials can be revealed only in logarithmic plots of resistivity versus reciprocal temperature.

Various laws describing the behavior of $\rho(T)$ in most cases can be considered as particular cases of the general relation

$$\rho(T) = A_0 \exp(\Delta_n/T)^{1/n}, \quad n = 1, 2, 3, 4.$$

For $n = 1$, this formula describes conductivity of a simple activation type with the activation energy Δ_1. The hopping conductivity of noninteracting electrons in disordered insulators and semiconductors at low temperatures obeys the Mott law ($n = 4$). This type of conductivity was observed in solid solutions $Fe_{1-x}V_xBO_3$ and in VBO_3 single crystals below room temperature. The value of $n = 2$ is indicative of a Coulomb interaction between localized electrons in a three-dimensional

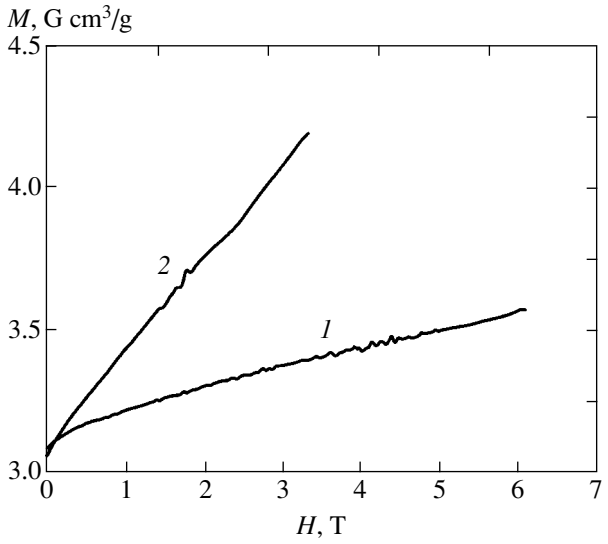

Fig. 5. The magnetization curves for $Fe_{1.91}V_{0.09}BO_4$ at T = 4.2 (*1*) and 100 K (*2*).

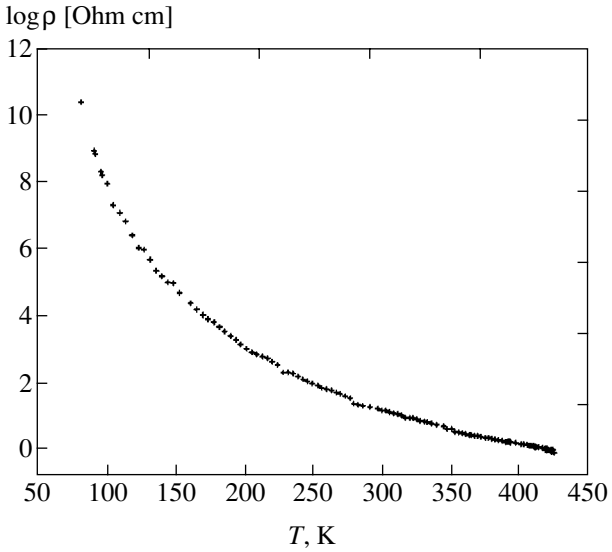

Fig. 6. The plot of logρ versus T for $Fe_{1.91}V_{0.09}BO_4$.

(3D) system. Efros and Shklovskii [17] showed that this interaction is manifested by the density of one-electron states tending to zero near the Fermi level. In this case, the resistance varies with the temperature as $\ln R \propto (\Delta_2/T)^{1/2}$, where

$$\Delta_2 \sim e^2/\varepsilon\zeta,$$

e is the electron charge, ε is the dielectric constant, and ζ is a linear size of localization.

According to [13], the conductivity of unsubstituted Fe_2BO_4 warwickite obeys a simple activation law with an activation energy of $\Delta_n \approx 0.33$ eV. Our investigation of the electric resistance of a $Fe_{1.91}V_{0.09}BO_4$ single crystal revealed deviation from the linear temperature dependence, $\ln\rho(T) \propto T^{-1}$. This behavior of the resistivity can be explained by the existence of various competitive mechanisms of electric conductivity. Least squares processing of the experimental data leads to the following empirical relation:

$$R(T) = A_1\exp(\Delta_1/T) + A_2\exp(\Delta_2/T)^{1/2},$$

where the coefficients A_1 and A_2 weakly depend on the temperature. The first term corresponds to a conductivity component with the simple activation character, while the second term describes the hopping of strongly correlated electrons (Fig. 7). The former activation energy is $\Delta_1 = 0.15 \pm 0.01$ eV. The Coulomb interaction energy amounts to $\Delta_2 = 4.92 \pm 0.01$ eV, which is characteristic of oxides.

Theoretical investigation of the electron structure of a natural warwickite of the $MgTiBO_4$ type [18, 19] showed that a correct description of the electron properties of this system requires taking into account electron correlations at the 3*d* metal sites. According to the results of these calculations, the Fermi level E_F is situated inside a *d* band of the transition metal, so that doping of such compounds can shift the E_F value toward the bandgap.

Having studied the electrical properties of unsubstituted compound Fe_2BO_4, Attfield *et al.* [20] suggested that the charge ordering in this crystal is also related to the Coulomb repulsion. A broad, weakly pronounced semiconductor–semiconductor transition (without significant change in the activation energy) observed at T = 317 K in Fe_2BO_4 [4] is not manifested in substituted compound $Fe_{1.91}V_{0.09}BO_4$ warwickite. However, it should be noted that the measurements reported in [4] were performed on polycrystalline samples and, hence,

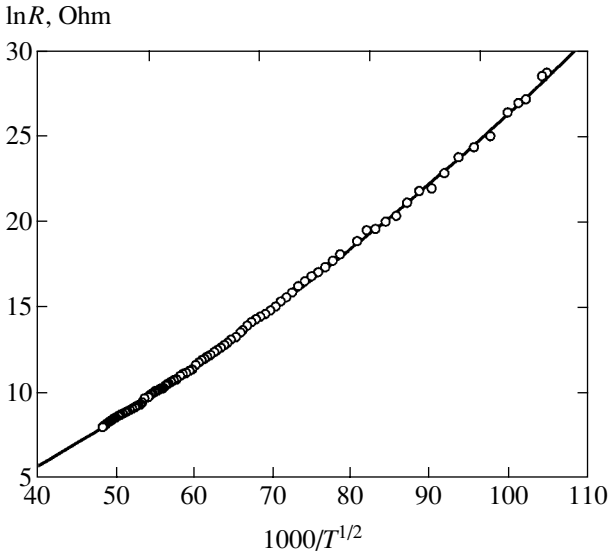

Fig. 7. The plot of ln$R$ versus $T^{-1/2}$ for $Fe_{1.91}V_{0.09}BO_4$.

the possible influence of grain boundaries should be borne in mind.

6. DISCUSSION OF RESULTS

Apparently, the magnetic and electrical properties of the new compound $Fe_{1.91}V_{0.09}BO_4$ differ from those of Fe_2BO_4, although one cannot speak of radical changes. The available experimental data reveal important features in common for Fe_2BO_4 and the new $Fe_{1.91}V_{0.09}BO_4$ warwickite:

(i) the orthorhombic structure at high temperatures; (ii) the existence of two nonequivalent crystallographic positions; (iii) the *P*-type ferrimagnetic ordering.

According to the neutron diffraction data for unsubstituted Fe_2BO_4, the structure of this warwickite represents a system of linear, weakly interacting ribbons, each comprising two internal and one external chains (Fig. 8). The $(M,M')O_6$ octahedra (edge-sharing) form infinite chains parallel to the short crystallographic *a* axis. The ribbons are linked by common vertices and trigonal BO_3 groups. Cations belonging to octahedra of the same ribbon interact via two oxygen atoms occupying vertices of the common edge. In this case, the M–O–M' angle approximately equals 90°, so that an indirect 90° exchange takes place inside each ribbon. The interaction between cations belonging to the adjacent ribbons is mediated by a single oxygen atom occupying the vertex shared by octahedra.

It can be suggested that, when a part of the iron ions are replaced by vanadium in the $Fe_{1.91}V_{0.09}BO_4$ crystal, the existing 3*D* magnetic structure is retained and also represents a system of substructures having the form of ribbons. The introduction of vanadium leads to an increase in the saturation magnetic moment, which can be related to a decrease in the absolute magnetization of sublattice II.

The results of our investigation showed that the introduction of vanadium leads to modification of the electrical properties of the system. To reveal the origin of these changes, let us compare the electron structures of Fe_2BO_4 and $Fe_{1.91}V_{0.09}BO_4$. These compounds are characterized by strong electron correlations in the narrow *d* bands, forming both local magnetic moments and the dielectric ground state. The presence of strong electron correlations hinders reliable calculations of the energy band structure by traditional one-electron methods of the band theory in the local electron density functional approximation.

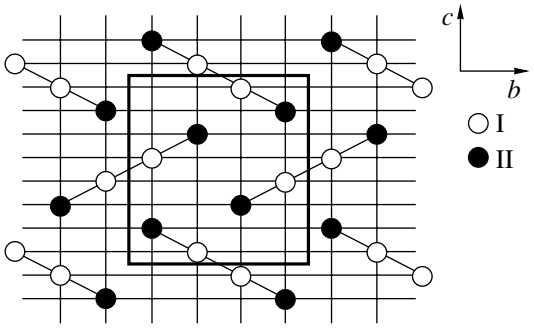

Fig. 8. A schematic diagram of the structure of $Fe_{1.91}V_{0.09}BO_4$ warwickite in a (100) plane: I and II are crystallographically nonequivalent cation positions.

For the related borate $FeBO_3$, the band structure was calculated using the local spin density functional [21] and in a generalized gradient approximation taking into account nonlocal corrections to the local density functional [22]. Unfortunately, the latter paper, devoted to pressure-induced changes in the lattice parameters and the magnetic state, presented neither the band structure proper nor the density $N(E)$ of one-electron states. For this reason, our considerations are based primarily on the results reported in [21] for the partial contributions to the density of one-electron states from various orbitals (B2*s*, B2*p*, O2*s*, O2*p*, and Fe3*d*). According to these calculations, the bottom of the empty conduction band (C) and the top of the valence band (V) are formed by the *s*-, *p*-hybrid states of B and O. A narrow *d* band of Fe is situated near the valence band top.

In the one-electron calculation, the Fermi level falls inside the *d* band and the crystal acquires metal properties. Allowance of the strong electron correlations leads to modification of the calculated local spin density functional [21], whereby the main effect consists in splitting of the *d* band into the filled lower Hubbard band (LHB) and the empty upper Hubbard band (UHB) separated by a large gap on the order of *U*, the intraatomic Coulomb matrix element. The typical value of *U* in 3*d* metals is about 5 eV.

The proposed model of the electron band structure of the unsubstituted Fe_2BO_4 crystal is depicted in Fig. 9a. Here, a dashed line above the LHB shows an acceptor impurity level accounting for the activation conductivity with the activation energy E_a. The charge carriers are represented by the conduction electrons from LHB.

Substituting vanadium for a part of iron leads to an increase in the degree of disorder in the crystal, which results in the appearance of a pseudogap with a mobility threshold ε_{c1} at the conduction band bottom and ε_{c2} at the valence band top. The Fermi level occurs in the region of localized states (Fig. 9b). As a result of the Coulomb interactions, the density of states at the Fermi level $N(\varepsilon_F)$ is zero [17]. In the case of one-electron states, the conductivity would obey the usual Mott law, $\ln\sigma(T) \propto (\Delta_4/T)^{1/4}$, characterizing thermally activated jumps of variable length. Since charge carriers at the valence band top are strongly correlated electrons, it is by no means surprising that the conductivity of $Fe_{1.91}V_{0.09}BO_4$ is closer to the Efros–Shklovskii law, $\ln\sigma(T) \propto (\Delta_2/T)^{1/2}$, where $\Delta_2 \sim e^2/\varepsilon\zeta$ [17] and ζ is the electron localization length. In our case, the localiza-

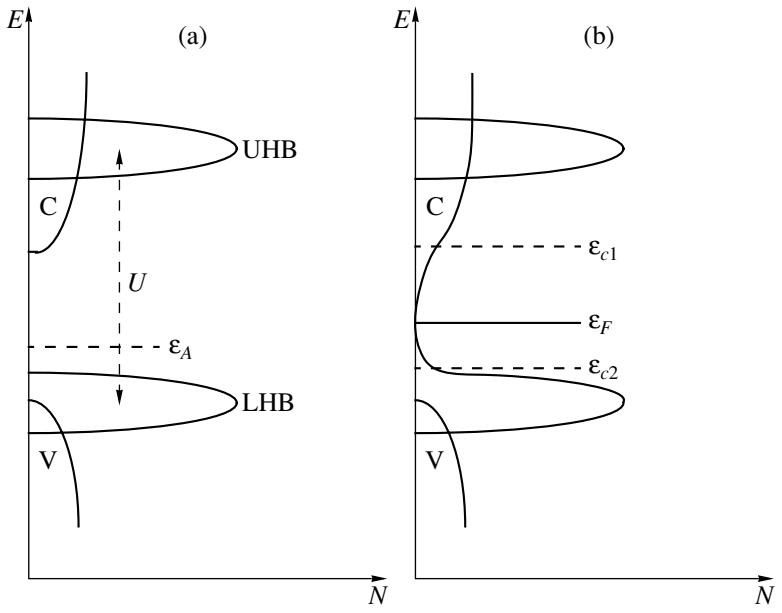

Fig. 9. A schematic energy diagram of the density of states for (a) Fe_2BO_4 and (b) $Fe_{1.91}V_{0.09}BO_4$ (see the text for explanations).

tion of 3*d* electrons is caused by the intraatomic strong electron correlations and it would be natural to assume that $\zeta \sim a_B$, where a_B is the Bohr radius, so that $\Delta_2 \sim U$.

The experimental results showed evidence for the existence of two competing mechanisms of conductivity, hopping and activation (with the activation energy Δ_1). This fact indicates that both localized electrons and band carriers are present in the system.

In conclusion, it should be noted that the $Fe_{1.91}V_{0.09}BO_4$ single crystals, in contrast to unsubstituted Fe_2BO_4, exhibit no structural transition. Adding vanadium significantly decreases the temperature of magnetic ordering, changes the type of conductivity, and alters the distribution of Fe^{2+}, $Fe^{2.5+}$, and Fe^{3+} cations over crystallographically nonequivalent positions.

ACKNOWLEDGMENTS

This study was supported in part by the Russian Foundation for Basic Research (project no. 03-02-16286) and by the Federal Program "Integration" (project no. B0017).

REFERENCES

1. J. C. Fernandes, R. B. Guimãraes, M. A. Continentino, *et al.*, Phys. Rev. B **50**, 16754 (1994).
2. R. B. Guimãraes, J. C. Fernandes, M. A. Continentino, *et al.*, Phys. Rev. B **56**, 292 (1997).
3. R. Norrestam, Z. Kristallogr. **189**, 1 (1989).
4. J. P. Attfield, A. M. T. Bell, L. M. Rodriguez-Martinez, *et al.*, J. Mater. Chem. **9**, 205 (1999).
5. M. A. Continentino, B. Boechat, R. B. Guimaraes, *et al.*, J. Magn. Magn. Mater. **226–230**, 427 (2001).
6. R. Norrestam, M. Kritikos, and A. Sjoerdin, J. Solid State Chem. **114**, 311 (1995).
7. M. J. Buerger and V. Venkatakrishnan, Mater. Res. Bull. **7**, 1201 (1972).
8. K. Bluhm and A. Utzolino, Z. Naturforsch. B **50**, 1450 (1995).
9. M. A. Continentino, J. C. Fernandes, R. B. Guimaraes, *et al.*, Philos. Mag. B **73**, 601 (1996).
10. B. Boechat, A. Saguia, and M. A. Continentino, Solid State Commun. **98**, 411 (1996).
11. A. Saguia, B. Boechat, and M. A. Continentino, J. Magn. Magn. Mater. **230**, 1300 (2001).
12. M. A. Continentino, A. M. Pedreira, R. B. Guimaraes, *et al.*, Phys. Rev. B **64**, 014406-1 (2001).
13. A. P. Douvalis, V. Papaefthymiou, A. Mookarika, *et al.*, J. Phys.: Condens. Matter **12**, 177 (2000).
14. A. P. Douvalis, V. Papaefthymiou, A. Mookarika, *et al.*, Hyperfine Interact. **126**, 319 (2000).
15. J. P. Attfield, J. F. Clarke, and D. A. Perkins, Physica B (Amsterdam) **180**, 581 (1992).
16. N. B. Ivanova, V. V. Rudenko, A. D. Balaev, *et al.*, Zh. Éksp. Teor. Fiz. **121**, 354 (2002) [JETP **94**, 299 (2002)].
17. A. L. Efros and B. I. Shklovskii, J. Phys. C **8**, L49 (1975).
18. M. Matos, R. Hoffmann, A. Latge, *et al.*, Chem. Mater. **8**, 2324 (1996).
19. D. C. Marcucci, A. Latge, E. V. Anda, *et al.*, Phys. Rev. B **56**, 3672 (1997).
20. J. P. Attfield, A. M. Bell, L. M. Rodriguez-Martinez, *et al.*, Nature **396**, 655 (1998).
21. A. V. Postnikov, St. Bartkowski, M. Neumann, *et al.*, Phys. Rev. B **50**, 14849 (1994).
22. K. Parlinski, Eur. Phys. J. B **27**, 283 (2002).

Translated by P. Pozdeev